Lattice Boltzmann algorithm for surface tension with greatly reduced microcurrents

S. V. Lishchuk, C. M. Care, and I. Halliday
Materials Research Institute, Sheffield Hallam University, Howard Street, Sheffield S1 1WB, United Kingdom
(Received 30 October 2002; published 11 March 2003)

We present an algorithm for inserting an interface between the immiscible phases of a multicomponent lattice Boltzmann fluid which is based solely upon the appropriate continuum physics: stress boundary conditions and continuity of velocity. Results are presented for the algorithm when applied to static, neutrally buoyant drops. It is shown that the present algorithm gives a significant reduction in the spurious velocities which are reported for previous schemes and a concomitant improvement in the isotropy of the interface.

DOI: 10.1103/PhysRevE.67.036701 PACS number(s): 02.70.−c, 47.11.+j

I. INTRODUCTION

A number of lattice Boltzmann equation (lBE) methods have been developed to deal with a wide range of continuum fluid applications [1]. An attraction of lBE is the intuitive way in which new physics can be inserted, as illustrated by the several fluid-fluid interface generating techniques which have been developed from the basic lBE algorithm. One area in which lBE is especially promising is complex fluids and, in particular, for immiscible liquid mixtures. In these systems one needs accurately to represent deformable interfaces separating immiscible components and the flow is typically at low Reynolds number and possibly with a complex geometry [2].

Surface tension may be activated by a number of possible methods [3–6], all of which are at some level physical and designed to imitate in varying degree, atomistic or *microscopic* behavior. Possibly as a result, the emergent continuum interface suffers from small and unwanted artifacts, principally (i) small, spurious velocities, or *microcurrents*, close to the interface, (ii) anisotropy in the effective surface tension (and hence boundary shapes), and (iii) a finite boundary thickness for the hydrodynamic regime. It should be noted that for correct hydrodynamics, immiscible liquids satisfy boundary conditions which obtain at a sharp, unstructured interface even at the mesoscale. However, lBE is a highly dispersive method and any interface algorithm based on local rules, for the sake of speed and computational simplicity, almost inevitably involves a degree of fluid mixing which distributes the emergent continuum interface. But while recognizing the need for speed, simplicity and stability, one must also recognize that to model continuum fluids with lBE, an interface should be as unstructured as possible. Accordingly, any interface generating algorithm which reduces microcurrents, such as we report here, and serves more sharply to define the interface is important for most applications.

It is true that more sophisticated model interfaces (e.g., Ref. [7]) are appropriate in applications where one seeks to capture, for example, the kinematics of phase separation [7]. But where hydrodynamics alone is the problem, ''simpler'' methods based directly upon mechanical quantities are acknowledged as being as valid [3,8]. Here we present a method for obtaining a direct interface between immiscible lattice fluids with the same density, although it is our intention to generalize this (density) aspect of the model in future work. It is important to note that the method presented here is based only on that physics which is appropriate for the length scale addressed in continuum hydrodynamics.

II. THEORY

A. The Gunstensen and Rothmann method

The arguments in this section are based upon the LBGK method which was pioneered by Qian and d'Humières [9], analyzed in detail by Hou *et al.* [10] and derived from the Boltzmann equation directly by He and Luo [11]. Results are presented in Sec. III to show that the new method is equally effective on D2Q7, D2Q9, and D2Q13 lattices and can be straightforwardly extended to three dimensions.

In the usual notation, the LBGK algorithm may be represented by the equation

$$f_i(\mathbf{r}+\mathbf{c}_i\delta_t, t+\delta_t) = f_i(\mathbf{r},t) + \frac{1}{\tau}(f_i^{(0)} - f_i) + F_i, \qquad (1)$$

where $\mathbf{c}_i$ represent the vectors of the lattice basis, δ_t represents the time step, and τ controls the molecular kinematic viscosity of the lattice fluid through the relation

$$\nu = \frac{2\tau - 1}{6}\delta_t, \qquad (2)$$

and the quantity F_i may be used to impress e.g., a pressure gradient. For the purposes of a Chapman-Enskog analysis, F_i is assumed to be introduced at $O(\delta_t)$. Velocity moments give the lattice fluid's density and momenta in the usual way through

$$\rho = \sum_i f_i = \sum_i f_i^{(0)},$$

$$\rho\,\mathbf{v} = \sum_i f_i\,\mathbf{c}_i = \sum_i \mathbf{c}_i f_i^{(0)}, \qquad (3)$$

where the equilibrium distribution function $f_i^{(0)}$ is

$$f_i^{(0)}(\rho,\mathbf{v}) = t_p\rho\left[1 + \frac{\mathbf{v}\cdot\mathbf{c}_i}{c_s^2} - \frac{|\mathbf{v}|^2}{2c_s^2} + \frac{(\mathbf{v}\cdot\mathbf{c}_i)^2}{2c_s^4}\right]. \qquad (4)$$

TABLE I. Data for different lattice types.

Lattice	t_0	t_1	t_2	c_s^2	α_M	$\left\|\frac{\alpha_M-\alpha}{\alpha}\right\|\times 100\%$
D2Q7	1/2	1/12		1/4	0.00706	8.5%
D2Q9	4/9	1/9	1/36	1/3	0.00722	6.5%
D2Q13	11/25	9/100	1/300	3/10	0.00757	1.9%

The weights t_p and the velocity of sound c_s are given in Table I. The form of the equilibrium distribution function, Eq. (4), ensures that relations (3) are satisfied and also determines the nonviscous part of the momentum-flux tensor of the lattice fluid,

$$\Pi^{(0)}_{\alpha\beta}=\sum_i f_i^{(0)}c_{i\alpha}c_{i\beta}=c_s^2\rho\delta_{\alpha\beta}+\rho v_\alpha v_\beta . \tag{5}$$

Gunstensen and Rothmann [3] proposed an extension to models such as those outlined above, using additional rules to confer spontaneous interface generation between *colored* momentum densities, now denoted by $R_i(\mathbf{r},t)$, $B_i(\mathbf{r},t)$. These component momentum densities undergo the collision part of the algorithm as a mixed, single density, as if it were *color blind*,

$$f_i(\mathbf{r},t)=R_i(\mathbf{r},t)+B_i(\mathbf{r},t). \tag{6}$$

A perturbation is then applied on those *mixed* nodes containing both red and blue densities, which has the effect of rendering the stress tensor anisotropic in such a way as correctly to recover a surface tension. Segregation of the two fluids then emerges upon the addition of a *recoloring* step for mixed nodes. Essentially the site totals of red and blue mass, $\rho_R(\mathbf{r},t)$ and $\rho_B(\mathbf{r},t)$ are conserved and reallocated to postcollision $f_i(\mathbf{r},t)$'s according to the following algorithm.

Where colors mix on the lattice, a color difference ρ^N is defined as

$$\rho^N(\mathbf{r},t)=\rho_R(\mathbf{r},t)-\rho_B(\mathbf{r},t) \tag{7}$$

in terms of which a color field may be calculated,

$$\mathbf{f}(\mathbf{x},t)=\nabla\rho^N. \tag{8}$$

The color field is approximately perpendicular to the interface and is used to define, n_α, a unit normal to the surface. To fourth-order accuracy, color field (8) is given by

$$\mathbf{f}(\mathbf{x},t)=\frac{1}{c_s^2}\sum_{ij} t_p\mathbf{c}_i[R_j(\mathbf{x}+\mathbf{c}_i,t)-B_j(\mathbf{x}+\mathbf{c}_i,t)]. \tag{9}$$

We note, in passing, that the inclusion of the factor t_p in definition (9) improves the definition of the color field as an interface normal; this minor point will be discussed in a future publication. The color is *demixed* relative to the color field, by reallocating color masses $\rho_R(\mathbf{r},t)$ and $\rho_B(\mathbf{r},t)$ over the postcollision "receptacle" $f_i(\mathbf{r},t)$'s so as to maximize the work done by color flux $\mathbf{q}(\mathbf{x},t)$,

$$\mathbf{q}(\mathbf{x},t)=\sum_i t_p\mathbf{c}_i[R_i(\mathbf{x},t)-B_i(\mathbf{x},t)] \tag{10}$$

against the color field [3]. Relaxation parameters τ with a limited range of difference may be applied in the bulk of the separated liquids, conferring different kinematic viscosities. In the mixing (interfacial) regions we use effective relaxation parameter τ_{eff}:

$$\nu_{eff}=\frac{1}{6}(2\tau_{eff}-1)=\frac{\rho_R}{\rho_R+\rho_B}\nu_R+\frac{\rho_B}{\rho_R+\rho_B}\nu_B . \tag{11}$$

B. New method

We now modify the Gunstensen algorithm by replacing the perturbation step with a direct forcing term at mixed sites, chosen so as to recover the required pressure difference across the interface. This recovers the macroscopic effects of surface tension in such a way as significantly to reduce the artifacts associated with earlier methods.

Consider mixing and demixing red and blue fluids, passively separated parallel to the direction of $\mathbf{f}(\mathbf{x},t)$, as above. Such a passive process will not affect the hydrodynamics of the combined fluids' mixture. Accordingly stress will be continuous throughout this region, which may be confirmed by direct measurement. We therefore assume that stresses measured on either side of a narrow red-blue interfacial region satisfy

$$\sigma^{(R)}_{\alpha\beta}t_\beta-\sigma^{(B)}_{\alpha\beta}t_\beta=0, \tag{12}$$

where, for example, $\sigma^{(R)}_{\alpha\beta}$ denotes the red fluid stress on the red side of the interface and t_β is a unit interfacial tangent, derived from the interface normal, through Eq. (8). If the red and blue fluids are each individually incompressible,

$$\partial_\beta v^{(C)}_\beta=0, \tag{13}$$

where $C=R$ or B. In three dimensions, the standard condition on the normal stress at the boundary between the fluids is given by [12]

$$\sigma^{(R)}_{\alpha\beta}n_\beta-\sigma^{(B)}_{\alpha\beta}n_\beta=\alpha\left(\frac{1}{R_1}+\frac{1}{R_2}\right)n_\alpha , \tag{14}$$

where α is a surface tension parameter and n_α is the local interfacial unit normal. This is equivalent to the requirement that the pressure must be distributed over the interface according to

$$P^{(1)}-P^{(2)}=\alpha\left(\frac{1}{R_1}+\frac{1}{R_2}\right). \tag{15}$$

In Eq. (14) R_1, R_2 are the local values of the principal radii of curvature of the interface. For a model with a continuous tangential stress, therefore, the task of forcing the correct condition of normal interfacial stress reduces to a requirement on a pressure difference ΔP related to the instantaneous local curvature through Eq. (15).

In order to impose results (14) and (15) onto the behavior of our lattice fluids we force a local pressure gradient throughout the (narrow but distributed) interface as an additional force density; i.e., the forcing is applied only on mixed sites of the lattice. In lBE, a body force can be impressed as an appropriate perturbation to the f_i's through the term F_i in Eq. (1) [13]. The necessary force is defined to act normal to the local interface, centripetally and with a magnitude proportional to the gradient in ρ^N/ρ. The local curvature of the interface, for a two-dimensional system, is given by

$$K=\frac{1}{R}=-\nabla_S\cdot\mathbf{n}, \tag{16}$$

where

$$\nabla_S=(\mathbf{I}-\mathbf{nn})\cdot\nabla, \tag{17}$$

I is the unit tensor, ∇_S is the surface gradient operator, and n is the interface normal, determined as the unit vector, parallel to the gradient of the color step function $\nabla(\rho^N/2\rho)$. In two dimensions, the curvature can be written as

$$K=n_x n_y(\partial_x n_y+\partial_y n_x)-n_y^2\partial_x n_x-n_x^2\partial_y n_y, \tag{18}$$

and can be evaluated by standard finite difference methods on the lattice. In order to impose condition (15), the momentum density $f_i(\mathbf{r},t)$ of the ith link in Eq. (1), must be augmented by

$$F_i=\frac{\alpha}{c_s^2 R}t_p c_{i\mu}\partial_\mu\left(\frac{\rho^N}{2\rho}\right). \tag{19}$$

Equation (19) includes the gradient of the color step function to ensure that, when considered as a line integral along the local normal, the cumulative effect of the body force is to produce an appropriate local step in pressure across the interface in accord with that prescribed in Eq. (15). This term is valid provided the fluid is incompressible. The perturbation is applied prior to the reallocation of color, as described in the text following Eq. (9). Note that in body forcing the lattice fluid, the stress field remains continuous. Note also that the total force on a drop, generated by a normal force of constant magnitude per unit length (the total color step across the interface should be uniform), should be zero, for a drop has a closed interface.

Before proceeding, it is perhaps appropriate to summarize, in broad terms, the algorithm in mixed regions of the lattice. At mixed (interfacial) nodes: (a) collide according to Eq. (1), (b) determine and apply body force (19), (c) reallocate colored densities ρ^R and ρ^B.

III. RESULTS

In this section, we test the interface algorithm described in Sec. II. In order to assess the algorithm we consider a static (red) drop and measure its isotropy (the uniformity of its radius with position on the interface) and the microcurrent activity it generates. The latter is measured after the manner outlined in Ref. [6]. In order to make sensible comparison with previous results we use lattices of identical size, drops of identical initial radius, surface tension parameter α, and an equivalent lattice closure process to those used in Ref. [6].

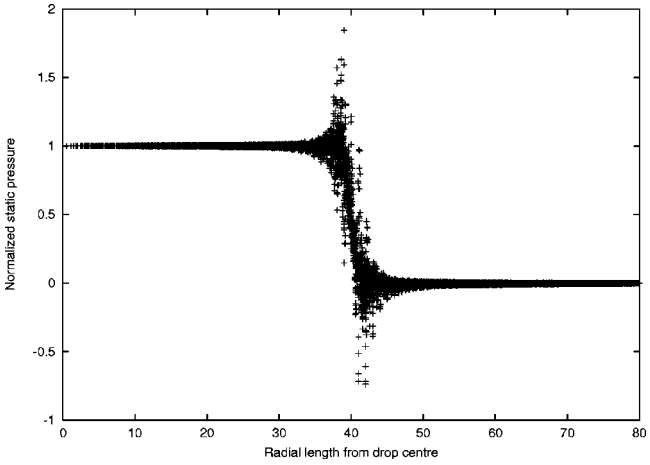

FIG. 1. Normalized pressure difference as a function of distance (lattice units) from the drop center.

The simulation was run on D2Q7, D2Q9, and D2Q13 lattices. The data were extracted after 10^5 time steps from a static drop on a 150×150 lattice with initial radius $R=40$, $\tau^{-1}=1.5$, and surface tension parameter $\alpha=0.007\,72$. Figure 1 plots the pressure $p=\rho/c_s^2$ against horizontal distance from an undeformed drop center. In the inner and outer regions of the drop the pressure is constant with good accuracy, and shows some variation in the interfacial region.

In order to obtain the macroscopic surface tension α_M we follow Eq. (15) and write

$$\alpha_M=R(\overline{p^R}-\overline{p^B}), \tag{20}$$

where $\overline{p^R}$ is the the mean static pressure inside the drop (averaged over all the points of radius $r\leqslant32$ lattice units

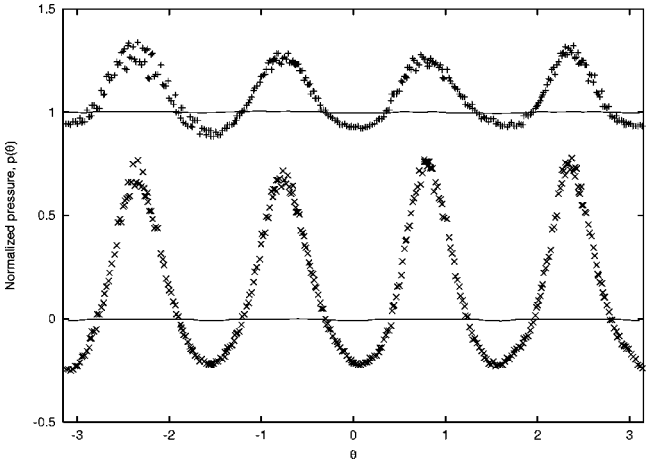

FIG. 2. Variation of normalized static fluid pressure p with rotational angle θ. Symbols ($+$ for the red fluid, $\times$ for the blue fluid) correspond to data from Ref. [6]; solid lines represent the results of the present work.

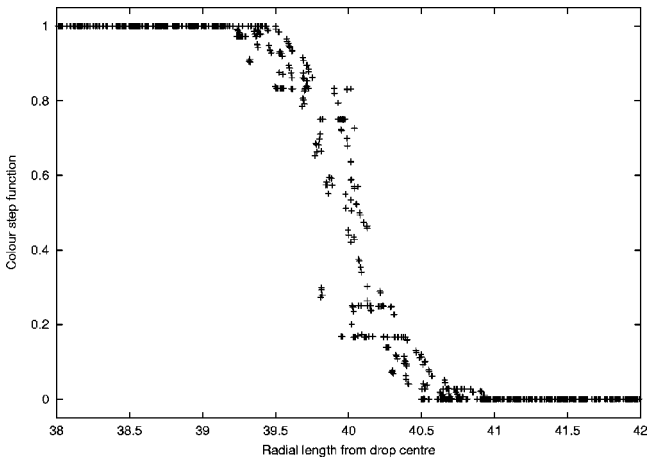

FIG. 3. Color interface location as a function of distance (lattice units) from the drop center.

from the drop center), $\overline{p^B}$ is the external mean pressure (averaged over all the points of radius $r \geqslant 48$), and the radius of the drop R is taken as the initialized radius of 40 lattice units. For the same drop, the recorded values of the standard Laplace surface tension, for all lattice types used, are close to the imposed surface tension parameter α (see Table I). The origin of the small discrepancy is the subject of current investigation, but does not in any way limit the applicability of the method.

The anisotropy of the surface tension, characterized by the variation of $p(R)$ and $p(B)$ with polar angle θ appears to be much smaller than that in the Gunstensen method (see Fig. 2). Additionally, the variations of the distance between the droplet center of mass and the interface with polar angle are not larger than the distance between adjacent nodes.

Figure 3 plots the color step function ρ^N/ρ against horizontal distance from an undeformed drop center in the vicinity of the interface. As in other diphasic LBGK algorithms, there is a small variation of density across the interfacial region having width 1–2 nodes. Hence, small drops ($R \leqslant 2$) may consist fully of mixed nodes and, as a result, show

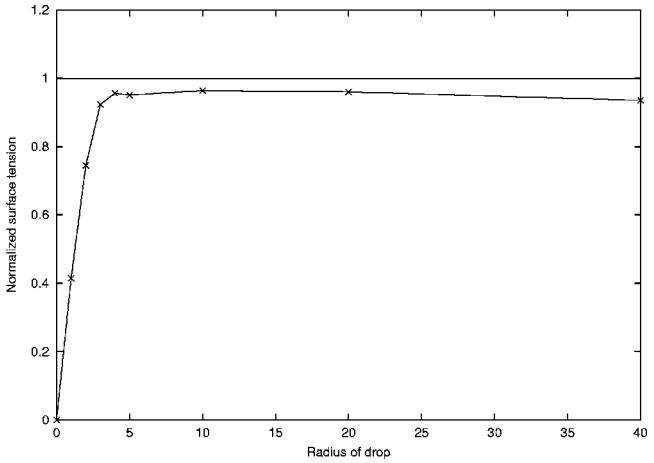

FIG. 4. Surface tension as a function of drop radius (lattice units). Data normalized by the surface tension parameter α.

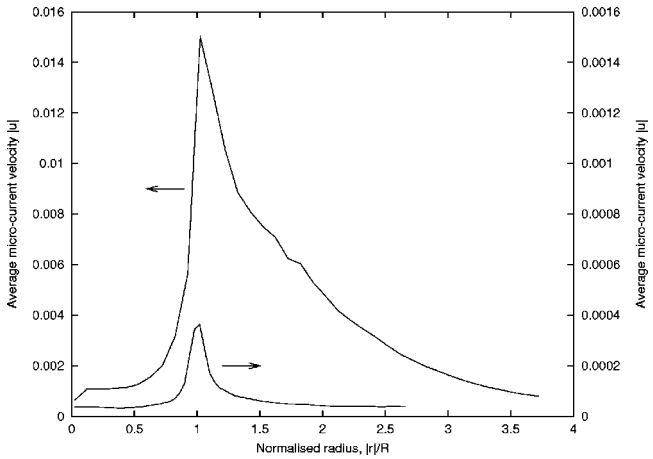

FIG. 5. Variation of $|\mathbf{u}|$, microcurrent flow speed measured in units of lattice spacing per time step, against normalized distance from the drop center, $|\mathbf{r}|/R$. The solid line corresponds to data from Ref. [6]; the dotted line corresponds to data obtained by the method described in the present work.

lesser pressure difference than it is expected from the Laplace law. For larger drops ($R > 2$) the macroscopic surface tension α_M calculated using Eq. (20) is close to the initial surface tension α, as it is seen from Fig. 4 where it is plotted for static droplet of different radii.

Figure 5 shows the radial variation of microcurrent velocity in D2Q9 lattice, mean square averaged over polar angle. The microcurrent velocity observed under the same conditions appears to be about 40 times smaller than that in Ref. [6]. Microcurrents are concentrated close to the interface and, moreover, decay faster in the bulk.

To demonstrate the applicability of the proposed method for the dynamic cases and to three dimensions, the simulation of the behavior of initially static three-dimensional drop in shear flow has been performed. A spherical drop of radius $R = 8$ was put in the center of the simulation box of size $40 \times 24 \times 24$. We used the D3Q19 lattice with a body force

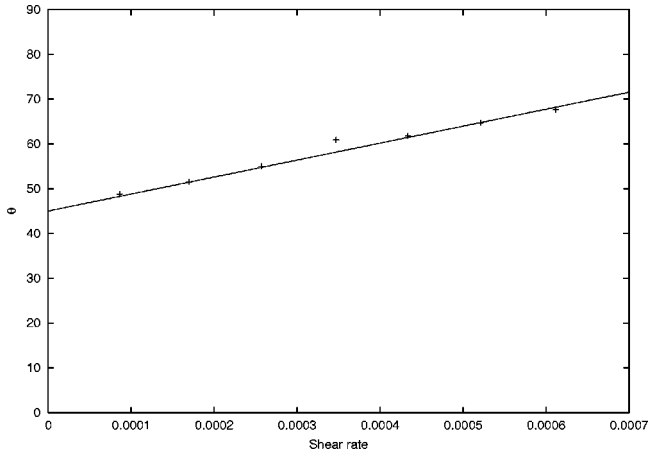

FIG. 6. Angle θ measured with respect to the direction of flow, of the principal axis of a three-dimensional droplet distorted by a shear flow. Shear rate in lattice units.

acting in the positive (negative) x direction applied to the nodes with the lowest (highest) y coordinate. The curvature was calculated using Eq. (18). At small shear rates the droplet distorts into an ellipsoid which is aligned with its major axis at an angle θ to the flow axis. Results are presented in Fig. 6 for the variation of θ and this is seen to intersect the θ axis at approximately 45°, as is expected from the theory. The small system size leads to the slightly noisy results shown in Fig. 6, and work in progress will report a more comprehensive comparison with the theory of Cox [14].

IV. CONCLUSIONS

This paper has reported a continuum surface tension generating algorithm for a two component lattice Boltzmann scheme, which exhibits a significant reduction in the artifacts which are present in many earlier schemes. The method has been validated for a number of two- and three-dimensional lattices and will be easily extended to situations where additional features, aimed at increasing separated fluids density difference, are present.

[1] S. Succi, *The Lattice Boltzmann Equation for Fluid Mechanics and Beyond* (Oxford University Press, New York, 2001).
[2] A. Koponen, M. Kataja, and J. Timonen, Int. J. Mod. Phys. C **9**, 1505 (1998).
[3] A.K. Gunstensen, D.H. Rothman, S. Zaleski, and G. Zanetti, Phys. Rev. A **43**, 4320 (1991).
[4] X.W. Shan and H.D. Chen, Phys. Rev. E **49**, 2941 (1994).
[5] M.R. Swift, W.R. Osborn, and J.M. Yeomans, Phys. Rev. Lett. **75**, 830 (1995).
[6] S.P. Thompson, I. Halliday, and C.M. Care, Phys. Chem. Chem. Phys. **1**, 2183 (1999).
[7] M.R. Swift, E. Orlandini, W.R. Osborn, and J.M. Yeomans, Phys. Rev. E **54**, 5041 (1996).
[8] M. Do-Quang, E. Aurell, and M. Vergassola, Tech. Rep., Uppsala University, Department of Scientific Computing, 2000.
[9] Y.H. Qian, D. d'Humieres, and P. Lallemand, Europhys. Lett. **17**, 479 (1992).
[10] Q. Zou, S. Hou, S. Chen, and G.D. Doolen, J. Stat. Phys. **81**, 319 (1995).
[11] X. He and L.-S. Luo, Phys. Rev. E **56**, 6811 (1997).
[12] L.D. Landau and E.M. Lifshitz, *Fluid Mechanics*, 6th ed. (Pergamon Press, New York, 1966).
[13] I. Halliday, S.P. Thompson, and C.M. Care, Phys. Rev. E **57**, 514 (1998).
[14] R.G. Cox, J. Fluid Mech. **37**, 601 (1969).